Journal of Neurochemistry

JOURNAL OF NEUROCHEMISTRY | 2009 | 109 | 360–370 doi: 10.1111/j.1471-4159.2009.05980.x

The N-terminal tripeptide of insulin-like growth factor-I protects against β-amyloid-induced somatostatin depletion by calcium and glycogen synthase kinase 3β modulation

Emma Burgos-Ramos,*,† Gabriel Á Martos-Moreno, *,†,‡ Manuela G. López,§ Rosario Herranz,¶ David Aguado-Llera,** Javier Egea,§ Diana Frechilla,†† Edurne Cenarruzabeitia,†† Rafael León,§ Eduardo Arilla-Ferreiro,** Jesús Argente*,†,‡ and Vicente Barrios*,†

*Department of Endocrinology, Hospital Infantil Universitario Niño Jesús, Madrid, Spain

†CIBER Fisiopatología Obesidad y Nutrición (CB06/03), Instituto de Salud Carlos III, Madrid, Spain

‡Department of Pediatrics, Universidad Autónoma de Madrid, Madrid, Spain

§Department of Pharmacology and Therapeutics, Universidad Autónoma de Madrid, Madrid, Spain

¶Instituto de Química Médica, CSIC, Madrid, Spain

**Neurobiochemistry Unit, Department of Biochemistry and Molecular Biology, Medical School, Universidad de Alcalá, Alcalá de Henares, Spain

††Department of Pharmacology and CIMA, University of Navarra, Pamplona, Spain

Abstract

The protective effects of insulin-like growth factor I on the somatostatin (SRIF) system in the temporal cortex after β-amyloid (Aβ) injury may be mediated through its N-terminal tripeptide glycine-proline-glutamate (GPE). GPE is cleaved to cyclo[Pro-Gly] (cPG), a metabolite suggested to mediate in neuroprotective actions. We evaluated the effects of GPE and cPG in the temporal cortex of Aβ25–35-treated rats on SRIF and SRIF receptor protein and mRNA levels, adenylyl cyclase activity, cell death, Aβ25–35 accumulation, cytosolic calcium levels ($[Ca^{2+}]_c$) and the intracellular signaling mechanisms involved. GPE and cPG did not change Aβ25–35 levels, but GPE partially restored SRIF and SRIF receptor 2 protein content and mRNA levels and protected against cell death after Aβ25–35 insult, which was coincident with Akt activation and glycogen synthase kinase 3β inhibition. In addition, GPE displaced glutamate from NMDA receptors and blocked the glutamate induced rise in cytosolic calcium in isolated rat neurons and moderately increased Ca^{2+} influx *per se*. Our findings suggest that GPE, but not its metabolite, mimics insulin-like growth factor I effects on the SRIF system through a mechanism independent of Aβ clearance that involves modulation of calcium and glycogen synthase kinase 3β signaling.

Keywords: calcium, glycogen synthase kinase 3β, Gly-Pro-Glu, neuroprotection, somatostatin, β-amyloid.

J. Neurochem. (2009) **109**, 360–370.

Alzheimer's disease (AD) is characterized by the presence of senile plaques containing β-amyloid (Aβ) and neuronal loss (Walsh and Selkoe 2004). The most frequent alteration of a neuropeptide in the brain of patients with AD is the reduction of somatostatin (SRIF), implicated in learning and memory, in the temporal cortex (Reinikainen *et al.* 1990). The effects of SRIF are mediated via five SRIF receptor subtypes located in diverse brain areas, including the temporal cortex. These

Received July 9, 2008; revised manuscript received January 19, 2009; accepted January 22, 2009.

Address correspondence and reprint requests to Vicente Barrios, Department of Endocrinology, Hospital Infantil Universitario Niño Jesús, Avda. Menéndez Pelayo, 65, E-28009 Madrid, Spain.
E-mail: vbarrios@telefonica.net

Abbreviations used: $[Ca^{2+}]_c$, cytosolic calcium; AC, adenylyl cyclase; AD, Alzheimer's disease; Aβ, β-amyloid; CREB, cAMP-responsive element binding protein; ECL, enhanced chemiluminescence; ERK, extracellular-signal regulated kinase; GPE, glycine-proline-glutamate; GSK3β, glycogen synthase kinase 3β; HSP27, heat-shock protein 27; IGF-I, insulin-like growth factor-I; PVDF, polyvinylidene fluoride; SDS, sodium dodecyl sulfate; SRIF, somatostatin; SRIF-LI, somatostatin-like immunoreactivity; sst, somatostatin receptor subtype; TTBS, Tween 20 Tris Buffered Saline; TUNEL, terminal deoxynucleotidyltransferase-mediated dUTP nick end labeling.

receptors are coupled, via G proteins, to different signal transduction pathways including inhibition of adenylyl cyclase (AC) (Reisine and Bell 1995). A marked loss of SRIF receptors with unaltered levels of Gi proteins has been reported in the cortex of AD patients (Cowburn *et al.* 1991).

Diverse approaches have been tested to block Aβ toxicity and diminish the progression of AD. Insulin-like growth factor-I (IGF-I) that acts as a survival factor in the brain, inhibits glycogen synthase kinase 3β (GSK3β) through phosphorylation on Ser9 in a PI3K-dependent manner preventing apoptosis (Quevedo *et al.* 2000). However, its use in AD is restricted given its limited ability to cross the blood–brain barrier and potential mitogenic effects (Górecki *et al.* 2007). IGF-I is cleaved in brain into des-(1–3)-IGF-I and the N-terminal tripeptide, glycine-proline-glutamate (GPE) (Sara *et al.* 1993) and this tripeptide is cleaved to cyclo[Pro-Gly] (cPG). The small size and stability of both compounds in the CNS make them good candidates for use in clinical therapies. Indeed, administration of GPE following ischemic brain injury reduces apoptosis and inhibits microglial proliferation (Guan *et al.* 2004) and cPG mediates memory processes.

However, there is little information regarding the effectiveness of GPE and cPG in protecting against Aβ induced damage. We have previously shown that GPE partially blocks Aβ-induced SRIF depletion in the temporal cortex (Aguado-Llera *et al.* 2004), although the mechanisms involved remain unknown. Aβ-induced cell death involves glutamate toxicity, resulting from over-activation of NMDA receptors and increased intracellular calcium (Hynd *et al.* 2004) and SRIF neurons are vulnerable to NMDA-receptor over-stimulation (Figueredo-Cardenas *et al.* 1994). Aβ-induced cell death is also dependent on GSK3β activation, through impairment of Akt signaling (Takashima 2006). Activity of GSK3β is regulated through phosphorylation (Grimes and Jope 2001) on serine (inhibitory) and tyrosine residues (stimulatory). Given that GPE can induce neuroprotection by acting as a NMDA receptor antagonist, reducing glutamate excitotoxic actions (Sara *et al.* 1993), we hypothesized that GPE and cPG may exert protective effects through modulation of cytosolic calcium levels ($[Ca^{2+}]_c$) and blockage of GSK3β signaling, thus reducing cell death and restoring SRIF levels in the temporal cortex of Aβ25–35-treated rats. To address this issue, we examined the effects of GPE and cPG after chronic Aβ25–35 administration on SRIF and SRIF receptor protein and mRNA levels, SRIF receptor binding capacity, as well as AC activity and αi1, αi2, and αi3 G protein concentrations in ovariectomized rats. This model was chosen because estrogens attenuate Aβ toxicity (Zheng *et al.* 2002).

In addition, we analyzed the effect of GPE and cPG treatments on Aβ-like immunoreactive levels, cell death and phosphorylation of Akt, GSK3β on Ser9 and Tyr216 residues, cAMP-responsive element binding protein (CREB), heat-shock protein 27 (HSP27), extracellular-signal regulated kinases 1/2 (ERK1/2), p38-MAPK and p53. Finally, the ability of GPE and cPG to modulate intracellular calcium signaling in isolated hippocampal neurons, NMDA binding and displacement of L-[^{3}H]glutamate from rat brain synaptic membranes and neuroprotection against NMDA excitotoxicity were also studied.

Experimental procedures

Chemicals and reagents

Synthetic [Tyr^{11}]-SRIF and SRIF-14 were purchased from Universal Biological (Cambridge, UK); carrier-free Na^{125}I (100 mCi/mL) and enhanced chemiluminescence (ECL) western blotting detection system from Perkin-Elmer Life Sciences (Boston, MA, USA) and GPE and cPG were from Bachem AG (Bubendorf, Switzerland). The antibody for the SRIF radioimmunoassay was raised in rabbits against SRIF-14. Antibodies against Aβ25–35 (A2275-76) and secondary antibody conjugated to horseradish peroxidase (I1906-10) were from United States Biological (Swampscott, MA, USA). Immobilon P^{SQ} membranes were purchased from Millipore (Bedford, MA, USA), polyvinylidene fluoride (PVDF) membranes and multiplex bead array assay kits from Bio-Rad Laboratories (Madrid, Spain) and osmotic minipumps from Alzet (Alza, Palo Alto, CA, USA). High-capacity cDNA archive kit, TaqMan PCR Master Mix and TaqMan gene expression assays were from Applied Biosystems (Foster City, CA, USA). fura-2AM was from Molecular Probes (Invitrogen, Carlsbad, CA, USA) and purchased from Invitrogen (Barcelona, Spain). Sigma (St Louis, MO, USA) was the source for all other reagents.

Animals and treatments

Thirty female Wistar rats (8 weeks of age) were bilaterally ovariectomized under anesthesia (0.1 mL of ketamine/kg wt and 0.2 mL of xylazine/kg wt). Three weeks after ovariectomy, animals were divided into six groups. Five rats were anesthetized and a cannula attached to an osmotic minipump was implanted into the right cerebral ventricle (−0.3 mm anteroposterior, 1.1 mm lateral from Bregma). Infusion of Aβ25–35 was administered during 14 days (300 pmol/day, infusion rate 0.5 μL/h), as described previously (Nag *et al.* 1999). The second and third experimental groups received Aβ25–35 at the same dose and for the same period of time and an intraperitoneal injection of 300 μg of GPE (Sizonenko *et al.* 2001) or cPG at 0, 6, and 12 days. The fourth and fifth groups of rats received GPE or cPG, as described above and an intracerebroventricular saline infusion during 14 days. Control ovariectomized rats received saline by the same routes. After treatment, the rats were killed by decapitation and the temporal cortex was dissected. The rats were treated according to the European Community laws for animal care and the experiment was approved by the Animal Care Committee of Alcalá University.

Immunoprecipitation and quantification of Aβ25–35

Aβ25–35 was immunoprecipitated according to the method of Williamson *et al.* (2002) with minor modifications. Briefly, immunoprecipitation was performed by incubation of tissue lysates

(100 μg total protein) with primary antibody (1 : 300) overnight at 4°C followed by addition of 50 μL protein A/G PLUS-agarose/mL and a further incubation of 4 h at 4°C. The mixture was then centrifuged at 14 000 *g* at 4°C for 15 s, and the supernatant was removed and stored at 4°C until analysis. The beads were washed three times in ice-cold ristocetin-induced platelet agglutination buffer and resuspended in 15 μL tricine buffer and boiled for 5 min.

Beta-amyloid-25–35 was resolved on a 15% (w/v) polyacrylamide sodium dodecyl sulfate (SDS)-Tris–Tricine gel. After separation, proteins were transferred onto PVDF membranes and blocked with Tween 20 Tris Buffered Saline (TTBS) containing 5% (w/v) bovine serum albumin for 1.5 h at 25°C. These membranes were incubated with the primary antibody at a dilution of 1 : 1000 in TTBS overnight at 4°C. The membranes were incubated with the secondary antibody at a dilution of 1 : 2000 in TTBS for 1.5 h at 25°C. The peptide was detected by an ECL system. Quantification was carried out by densitometry using a Gel Logic 1500 Imaging System (Kodak, Madrid, Spain).

SRIF radioimmunoassay

Somatostatin was extracted from temporal cortical tissue in 2 M acetic acid by homogenization and boiling during 5 min and measured by radioimmunoassay (Patel and Reichlin 1978).

Binding assay

Membranes from the temporal cortex were prepared (Reubi *et al.* 1981) and SRIF binding was measured in these membranes (0.15 mg protein/mL) incubated with 250 pM of ^{125}I-[Tyr^{11}]-SRIF in the absence or presence of 0.01–10 nM unlabelled SRIF during 60 min at 30°C.

Adenylyl cyclase assay

Adenylyl cyclase activity was measured in membranes (0.06 mg/mL) incubated with 1.5 mM ATP, 5 mM $MgSO_4$, 10 μM GTP, an ATP-regenerating system, 1 mM 3-isobutyl-1-methylxanthine, 0.1 mM phenylmethylsulfonyl fluoride, 1 mg/mL bacitracin, 1 mM EDTA, and 10^{-4} M SRIF. After a 15 min incubation at 30°C, the reaction was stopped by heating. After cooling, 0.2 mL of an alumina slurry (0.75 g/mL in Tris/HCl buffer, pH 7.4) were added and the suspension was centrifuged. The supernatant was used for assay of cAMP (Gilman 1970).

Western blotting

Fifty milligrams of temporal cortex were homogenized in a lysing solution (Bio-Rad Laboratories) following the manufacturer's instructions. The tissue lysates for pSer9-GSK3β, pTyr216-GSK3β, GSK3β, p-CREB, and CREB and the membrane extracts for somatostatin receptor subtype (sst) 1–4 and the αi1-3 G protein subunits were diluted in SDS-sample buffer. The proteins (30 μg for GSK3β, 60 μg for CREB and 100 μg for sst1–4 and αi1-3 G protein subunits) were run on a 10% SDS-polyacrylamide gel except for GSK3β forms that were run on an 8% gel. After separation, the proteins were transferred onto PVDF membranes and blocked with TTBS containing 5% (w/v) non-fat dry milk for 1.5 h at 4°C. These membranes were incubated with the primary antibodies (all diluted at 1 : 1000): rabbit anti-p-CREB, anti-CREB, anti-pSer9-GSK3β (Cell Signaling Technology, Danvers, MA, USA), mouse anti-pTyr216-GSK3β, anti-GSK3β (BD Transduction Labs, Franklin Lakes, NJ, USA), rabbit anti-αi1-2 monoclonal antibodies (Chemicon International, Temecula, CA, USA) or goat anti-sst1–4 and rabbit anti-αi3 polyclonal antibodies (Santa Cruz Biotechnologies, Santa Cruz, CA, USA) in TTBS overnight at 4°C. The membranes were incubated with the corresponding secondary antibody conjugated with peroxidase at a dilution of 1 : 2000, except for GSK3β at 1 : 10 000 dilution) in TTBS was added and incubated for 60 min. The proteins were detected by an ECL system.

Multiplex bead array assays

Phosphorylated forms of Akt, ERK1/2, p38-MAPK, HSP27 and p53 and total content of Akt and p38-MAPK were measured as previously described (Khan *et al.* 2004). Briefly, beads conjugated to the appropriate antibodies and tissue lysates (50 μL each) were incubated for 18 h at 25°C. Wells were washed using a vacuum manifold and antibody conjugated to biotin (25 μL) was added. After incubation for 30 min at 25°C, beads were incubated during 30 min with 50 μL streptavidin conjugated to phycoerythrin. Beads were analyzed in the Bio-Plex suspension array system 200 (Bio-Rad Laboratories). Raw data (mean fluorescence intensity) were analyzed using the Bio-Plex Manager Software 4.1 (Bio-Rad Laboratories).

RNA extraction, reverse transcription and RT-PCR for SRIF and SRIF receptors

Total RNA was extracted according to the Tri-Reagent protocol (Chomczynski 1993). The reverse transcription reaction and real-time PCR were performed on 50 ng of total RNA as previously reported (Aguado-Llera *et al.* 2007). Sequences of primers and probes for sst1, sst3, and sst4; as well as for glyceraldehyde-3-phosphate dehydrogenase, used as an invariant endogenous control for relative gene expression comparisons, have been reported (Aguado-Llera *et al.* 2007). According to the manufacturer's guidelines, the $\Delta\Delta C_T$ method was used for relative quantification. Statistics were performed using ΔC_T values.

Cell death detection

Detection of cell death was performed by a commercial ELISA kit, according to the manufacturer's protocol (Roche Diagnostics, Penzberg, Germany). Measurements were taken at 405 nm with an automatic microplate analyzer (Bio-Tek Instruments Inc., Winooski, VT, USA).

TUNEL/immunohistochemistry

Terminal deoxynucleotidyltransferase-mediated dUTP nick end labeling (TUNEL) and immunohistochemistry were performed as previously reported (Aguado-Llera *et al.* 2007).

Isolation and culture of rat hippocampal neurons

Pregnant rats were killed and 18-day old embryos were removed. Hippocampi were dissected under a stereomicroscope in phosphate-buffered saline at 4°C. The tissue was digested with 0.5 mg/mL papain and 0.25 mg/mL Dnase dissolved in Ca^{2+}- and Mg^{2+}-free phosphate-buffered saline containing 1 mg/mL bovine serum albumin and 6 mM glucose at 37°C for 20 min. The papain solution was replaced by 5 mL of Neurobasal medium

supplemented with 10% fetal bovine serum. The digested tissue was disaggregated and the cell suspension centrifuged for 4 min at 120 g. Cells were resuspended in 5 mL Neurobasal medium and plated at a density of 1×10^5 cells/mL on 4 cm diameter Petri dishes (2 mL per dish) coated with poly-D-lysine (0.1 mg/mL). Cells were plated in Neurobasal medium supplemented with 10% fetal bovine serum, 50 μg/mL streptomycin–penicillin and 50 μg/mL gentamicin, and maintained in an incubator at 37°C with 5% CO_2. After 24 h, the medium was replaced by fresh serum-free medium containing B27 supplement, essential for hippocampal neuronal survival. Under these conditions, standard cell survival was 4 weeks; the experiments were performed on neurons after 14–16 days in culture.

Binding to NMDA receptors

Cortical membranes were prepared according to the method of Foster and Fagg (1987). Displacement assays of glutamate with GPE and cPG from NMDA receptors were performed according to the method of Monahan and Michel (1987).

Neuroprotection against NMDA excitotoxicity

After 2 weeks, hippocampal neurons were loaded with Locke solution. After pre-incubation at 37°C with 10 μM GPE or cPG in Locke solution, exposure to NMDA was carried out for 3 h and neurons are maintained in an incubator at 37°C with 5% CO_2 (Snider *et al.* 2003). After this period, the medium was replaced by Neurobasal medium containing 10 μM GPE or cPG. Cell death was analyzed 24 after the beginning of the exposure period by measuring lactate dehydrogenase present in the medium (Koh and Choi 1987).

Cytosolic calcium measurements with fura-2

After 2 weeks post-plating, hippocampal neurons (2×10^5 cells/25 mm diameter dishes) were loaded with 3 μM fura-2/AM plus pluronic acid 0.02% for 45 min at 37°C in Krebs-HEPES solution containing (in mM): 140 NaCl, 5.6 KCl, 1.2 $MgCl_2$, 2 $CaCl_2$, 10 HEPES, 11 D-glucose, pH 7.4. Loading with fluorescent dye was terminated by washing the cells twice with Krebs-HEPES and then kept at 25°C for 15 min. Fluorescence was measured in a Nikon eclipse TE-300 microscope equipped with shutter lambda 10-2 filter wheels (Shutter instruments Co., Novato, CA, USA). fura-2 was excited at 340 and 380 nm. Emitted light was transmitted through a 405-nm dichroic mirror and a 500- to 545-nm barrier filter before being detected by a Hamamatsu cooled CCD-camera Orca-G (Hamamatsu Photonics Inc., Hirakuchi, Japan). $[Ca^{2+}]_c$ was calculated according to Grynkiewicz *et al.* (1985). Data were analyzed using the Metafluor v 2.2 Imaging System (Molecular Devices).

Statistical analyses

The LIGAND software (Bethesda, MD, USA) was used to analyze the binding data. This program was used to produce Scatchard plots and to compute values for receptor affinity (K_d) and density (B_{max}) that best fit the binding data. Statistical analysis was carried out by one-way ANOVA followed by a Scheffé *F*-test. Relationships between variables were determined by linear regression analysis. The values were considered significantly different when the p value was < 0.05. Statistical analyses were performed using Statview software (Statview 5.01; SAS Institute, Cary, NC, USA).

Results

GPE or cPG treatments did not change Aβ25–35 levels

To determine whether the IGF-I metabolites GPE and cPG alter Aβ-like immunoreactive levels, western blot was used. Aβ25–35 levels in the temporal cortex were not modulated by GPE or cPG treatment in either control rats or rats treated with Aβ25–35 (Fig. S1).

GPE, but not cPG, partially restored Aβ25–35-induced SRIF content and SRIF receptor density depletion

Continuous infusion of Aβ25–35 reduced SRIF-like immunoreactivity (SRIF-LI) content. GPE treatment, but not cPG, partially inhibited the loss of SRIF-LI in Aβ25–35-treated rats, whereas GPE or cPG had no effect in controls (Table 1).

Table 1 Effect of β-amyloid-25–35, Aβ25–35 plus Gly-Pro-Glu, Aβ25–35 plus cyclo[Pro-Glu], and GPE or cPG alone on somatostatin-like immunoreactivity levels and relative SRIF mRNA content, equilibrium parameters for ^{125}I-[Tyr^{11}]-SRIF binding in membranes from the temporal cortex and relative SRIF receptor subtype 2 protein and mRNA content

	SRIF-LI	SRIF mRNA	K_d	B_{max}	sst2	sst2 mRNA
Control	30.3 ± 5.2	100.0 ± 9.8	0.56 ± 0.03	538 ± 20	100.0 ± 2.7	100.0 ± 7.9
Aβ25–35	17.8 ± 3.2*	62.3 ± 15.7*	0.53 ± 0.02	356 ± 14*	59.8 ± 3.6*	60.3 ± 8.1*
Aβ25–35 + GPE	24.6 ± 2.9*#	83.2 ± 9.0*#	0.50 ± 0.05	465 ± 19*#	82.3 ± 4.8*#	79.5 ± 8.6*#
Aβ25–35 + cPG	19.4 ± 2.7*	67.0 ± 6.2*	0.55 ± 0.05	329 ± 22*	56.0 ± 6.0*	70.0 ± 12.5*
GPE	28.5 ± 3.8	96.2 ± 9.1	0.48 ± 0.03	511 ± 12	104.7 ± 4.2	102.3 ± 9.7
cPG	31.0 ± 2.5	106.2 ± 4.9	0.60 ± 0.06	520 ± 19	96.3 ± 5.0	90.9 ± 10.0

SRIF-LI is expressed in ng/mg protein. Binding parameters were calculated from Scatchard plots by linear regression. K_d is the dissociation constant expressed in nM; B_{max} is the maximum binding capacity expressed in fmol/mg protein; SRIF and sst2 mRNA levels are expressed as percentage of control densitometry units (DU). Values are expressed as the mean ± SEM. The number of rats in each experimental group was five. *$p < 0.05$ compared to C-Ovx group, #$p < 0.05$ compared to Aβ25–35-treated group.

Aβ25–35, β-amyloid-25–35; GPE, Gly-Pro-Glu; cPG, cyclo[Pro-Glu]; SRIF-LI, somatostatin-like immunoreactivity; sst2, SRIF receptor subtype 2.

Beta-amyloid-25-35 administration reduced the density of SRIF receptors. GPE, but not cPG, partially inhibited the Aβ25–35 induced reduction in the density of these receptors in the temporal cortex (Table 1). The affinity of the SRIF receptors was consistently unchanged in all groups. Treatments with GPE or cPG alone had no effect on these parameters.

To test if GPE or cPG had an effect on a specific receptor subtype, western blot analyses of sst1–4 were performed in membranes from the rat temporal cortex. A decrease in sst2 protein levels was found in the Aβ25–35-treated group, whereas GPE partially restored the loss of this receptor subtype. CycloPG did not restore the decrease of sst2 levels and neither compound alone had an effect on this parameter in controls (Table 1). Protein levels of sst1, sst3, or sst4 were consistently unchanged in all the experimental groups (data not shown).

Effect of GPE on AC activity

No significant differences in basal AC activity were detected among groups (data not shown). Basal AC activity was inhibited by SRIF in all experimental groups. However, the capacity of SRIF to inhibit AC activity in these membranes was different between groups (30.8 ± 1.1, 18.4 ± 1.8, 26.0 ± 1.0, 21.2 ± 1.1, 31.9 ± 1.6, and 30.1 ± 1.4, expressed as percent of SRIF inhibition of AC activity in control, Aβ25–35, Aβ25–35 plus GPE, Aβ25–35 plus cPG, GPE and cPG groups, respectively). The capacity of SRIF to inhibit this activity was significantly lower (40.2%, $p < 0.01$) in the Aβ25–35-treated group compared to controls. GPE, but not cPG treatment partially reduced the effect of Aβ25–35 on this parameter (15.6% less than controls, $p < 0.01$).

Gi proteins were unchanged by Aβ25–35, GPE or cPG treatments

Western blot analyses showed no differences in the levels of αi1 (100.0 ± 3.4, 91.3 ± 11.7, 92.6 ± 1.8, 106.0 ± 4.5, 110.3 ± 3.5, and 103.8 ± 2.9, expressed as percentage of densitometry units in control, Aβ25–35, Aβ25–35 plus GPE, Aβ25–35 plus cPG, GPE and cPG groups, respectively), αi2 (100.0 ± 0.8, 101.3 ± 6.0, 97.5 ± 0.2, 91.7 ± 4.7, 99.9 ± 2.7, and 101.8 ± 2.6) or αi3 (100.0 ± 1.7, 100.3 ± 4.6, 96.0 ± 6.0, 92.1 ± 6.3, 98.6 ± 2.5, and 95.1 ± 3.1) among the experimental groups.

GPE protected against the Aβ25–35-induced decrease in SRIF and sst2 mRNA levels

We found that SRIF and sst2 mRNA levels were significantly decreased in Aβ25–35 treated rats. GPE treatment of Aβ25–35-treated rats partially restored SRIF and sst2 mRNA levels, whereas cPG coadministered with Aβ25–35 and GPE or cPG alone had no effect on these levels (Table 1). No differences in the mRNA levels of sst1, sst3, or sst4 were found between the experimental groups (data not shown).

GPE treatment decreased Aβ25–35-induced cell death

Cell death was increased in the temporal cortex of Aβ25–35-treated rats and GPE partially inhibited the Aβ25–35 induced death. CycloPG did not modify cell death in Aβ25–35-treated rats. GPE or cPG alone had no effect on cell death (Fig. 1a).

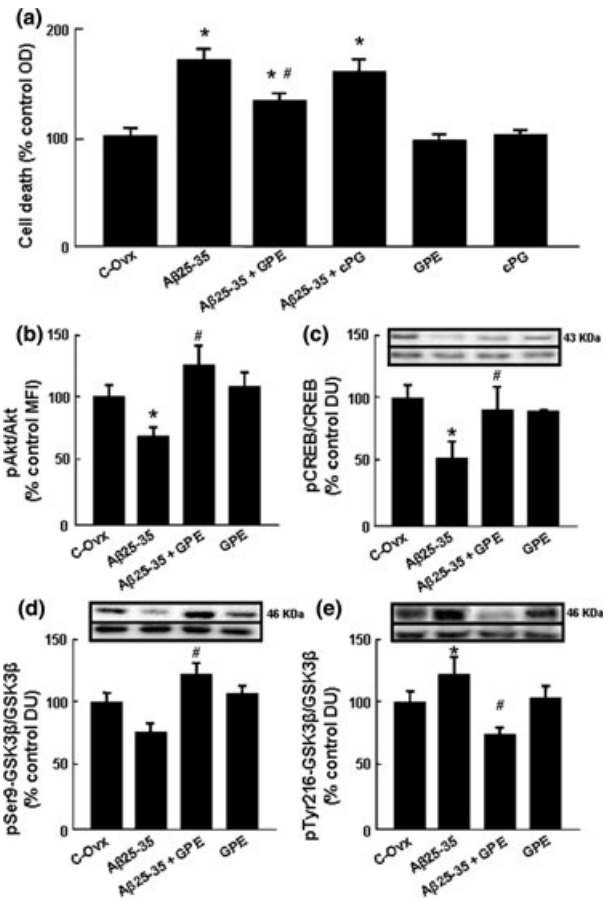

Fig. 1 (a) Relative cell death, as determined by ELISA, in the temporal cortex from control ovariectomized (C-Ovx) rats, C-Ovx rats treated with β-amyloid 25–35 peptide (Aβ25–35), C-Ovx rats treated with Aβ25–35 plus Gly-Pro-Glu (Aβ25–35 + GPE), C-Ovx rats treated with Aβ25–35 plus cyclo[Pro-Glu] (Aβ25–35 + cPG), C-Ovx rats treated with GPE alone and C-Ovx rats treated with cPG alone. Values represent the mean ± SEM of five rats. (b) Relative phosphorylated (p)-Akt protein levels [(MFI) of p-Akt/MFI of total Akt] in the temporal cortex of the same experimental groups, (c) Relative p-cAMP-responsive element binding protein (p-CREB) concentrations in the temporal cortex of the same groups, (d) Relative glycogen synthase kinase 3β phosphorylated on serine 9 (pSer9-GSK3β) protein levels in the temporal cortex of the same groups and (e) Relative glycogen synthase kinase 3β phosphorylated on tyrosine 216 (pTyr216-GSK3β) protein levels in the temporal cortex of the same groups. For quantification, p-CREB was normalized against total CREB and pSer9-GSK3β and pTyr216-GSK3β were normalized against total GSK3β. The data are expressed as a percentage of the control ratio. DU, densitometry units; MFI, median fluorescence intensity; MW, molecular weight. $^{*}p < 0.05$ compared to C-Ovx group, $^{\#}p < 0.05$ compared to Aβ25–35-treated group.

Few TUNEL-positive cells were detected in the control group (Fig. S2a). Increased TUNEL labeling was detected in Aβ25–35-treated rats (Fig. S2b) and GPE co-administration reduced the number of TUNEL positive cells (Fig. S2c). GPE alone did not change the number of TUNEL-positive cells (Fig. S2d).

Immunohistochemistry for SRIF was performed in conjunction with TUNEL labeling to identify cells undergoing apoptosis. Figure S2, panels f–h illustrates the colocalization of SRIF-immunopositive cells with TUNEL staining in Aβ25–35-treated rats.

Effect of GPE co-administration to Aβ25–35-treated rats on modulation of Akt, CREB and GSK3β signaling

β-amyloid activates GSK3 through inhibition of Akt signaling (Takashima 2006). Activation of Akt in the temporal cortex was reduced in Aβ25–35-treated rats and concomitant GPE treatment normalized Akt activation, whereas GPE alone had no effect (Fig. 1b). CycloPG did not revert the reduction in Aβ25–35-treated rats (78.3 ± 10.8 and 68.4 ± 3.5, expressed as percent of controls, in Aβ25–35 plus cPG and cPG groups, respectively) and cPG alone had no effect. Levels of pSer9-GSK3β were decreased and pTyr216-GSK3β increased in Aβ25–35-treated rats and GPE treatment return to normal values these levels (Fig. 1d, e).

Immunoblots of p-CREB showed that Aβ25–35 decreased the levels of p-CREB and GPE co-administration normalized p-CREB protein levels, whereas GPE administration to control ovariectomized rats had no effect (Fig. 1c). The total amount of CREB protein was not significantly altered by any of the treatments.

Analyses of activation of HSP27, p53, p38-MAPK, and ERK1/2 showed no significant differences between groups: HSP27 (100.0 ± 6.4, 100.6 ± 14.5, 86.1 ± 9.1, and 91.7 ± 14.2, expressed as percentage of mean fluorescence intensity in control, Aβ25–35, Aβ25–35 plus GPE or GPE groups, respectively), p53 (100.0 ± 9.7, 93.0 ± 5.7, 84.9 ± 7.5, and 83.4 ± 10.7), p38-MAPK (100.0 ± 10.9, 97.0 ± 12.6, 111.2 ± 10.2, and 117.4 ± 12.5) and ERK1/2 (100.0 ± 9.5, 112.8 ± 11.6, 101.2 ± 8.4, and 113.8 ± 5.7). Total protein levels of these factors were not affected by any of the treatments.

Effects of GPE and cPG on glutamate displacement from NMDA receptors and neuroprotection against NMDA excitotoxicity

Displacement of L-[^{3}H]glutamate from NMDA receptors by GPE showed a K_i of 31.2 ± 15.7 μM, whereas no displacement was found using concentrations up to 100 μM of cPG.

The neuroprotective effects were evaluated in cultured hippocampal neurons exposed to NMDA (10 μM). GPE decreased NMDA induced cell death by 26.8% ± 3.5% ($p < 0.01$), whereas cPG did not exhibit this property (1.4% ± 0.1%, non-significant).

GPE reduced the glutamate-induced $[Ca^{2+}]_c$ rise in hippocampal neurons

To determine if GPE modulates glutamate signaling we conducted the following experiments. In fura-2 loaded hippocampal neurons, the increase in $[Ca^{2+}]_c$ induced by 2 s pulses of 100 μM glutamate in the presence of glycine 10 μM was measured. Control pulses, in the absence of GPE, gave a fura-2 ratio of approximately one (Fig. 2a). After a control pulse, cells were incubated with GPE for 2 min. Subsequent depolarization with glutamate reduced the fluorescent signal with respect to the control pulse. Following 1 min washout of the compounds, neurons tended to recover the signal induced by glutamate. The peak calcium signal

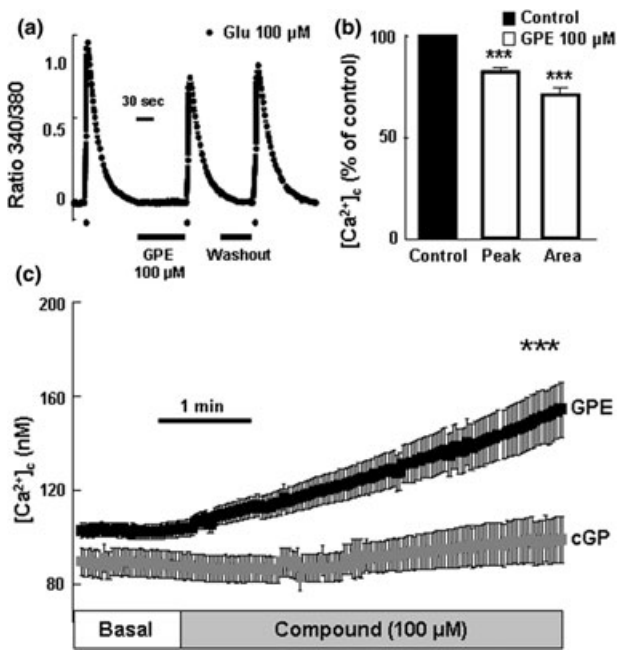

Fig. 2 Inhibitory effect of GPE on the glutamate (100 μM) induced elevation of $[Ca^{2+}]_c$ in cultured hippocampal neurons. $[Ca^{2+}]_c$ was measured in fura-2/AM loaded hippocampal cells and data are reported as the ratio of emission at excitation wavelengths 340 and 380 nm. (a) Original recording of $[Ca^{2+}]_c$ elevation induced by 2 s pulses of 100 μM glutamate in the absence or presence of GPE (100 μM). Cells were incubated with GPE for 2 min before glutamate perfusion followed by 1 min washout with Krebs-HEPES solution. Fluorescence was monitored every 2 s. (b) Representation of the mean maximum $[Ca^{2+}]_c$ peak induced by glutamate in the presence or absence of GPE and mean total calcium entry measured as the area under the curve induced by glutamate. Data are normalized respect to the control signals before GPE incubation. Results are expressed as the mean ± SEM of 14 cells of three different cultures. ***$p < 0.001$ compared to control. (c) Effect of Gly-Pro-Glu (GPE) and cyclo[Gly-Pro] (cPG) on $[Ca^{2+}]_c$. $[Ca^{2+}]_c$ was measured in fura-2/AM loaded hippocampal cells and data are reported as concentration in nM. Cells were perfused with 100 μM GPE or cPG for 4 min and fluorescence was monitored every 2 s. Results are expressed as the mean ± SEM of 39 GPE- and 38 cPG-treated cells. ***$p < 0.001$ compared to cPG.

induced by glutamate was significantly reduced by GPE (15.9%). When total calcium entry was evaluated by calculating the area under the curve induced by glutamate, GPE decreased calcium entry by 19.7% (Fig. 2b). These results indicate that GPE reduces glutamate induced calcium entry.

Exposure to GPE induced a gradual increase of $[Ca^{2+}]_c$ in hippocampal neurons

To analyze if GPE or cPG could cause changes in the $[Ca^{2+}]_c$ *per se*, we performed the following assay. After stabilization of the basal $[Ca^{2+}]_c$, hippocampal neurons were continuously perfused for 4 min with 100 μM GPE or cPG and $[Ca^{2+}]_c$ were monitored every 2 s. GPE causes a gradual increment of $[Ca^{2+}]_c$, reaching values of approximately 140–150 nM. However, cPG had no significant effect on the $[Ca^{2+}]_c$ (Fig. 2c).

Effect of GPE on the $[Ca^{2+}]_c$ increase induced by depolarization with high $[K^+]$ in hippocampal neurons

To evaluate if GPE could modify calcium signaling mediated by cell depolarization we performed experiments in fura-2 loaded cells stimulated with depolarizing concentrations of K^+. When hippocampal neurons were continuously perfused with Krebs-HEPES solution and challenged with a solution containing 70 mM K^+ for 5 s, a transient $[Ca^{2+}]_c$ signal was recorded as an increase in the fura-2 340/380 ratio. Four consecutive 5 s pulses of 70 mM K^+ every 4 min gave $[Ca^{2+}]_c$ transients that gradually decayed (Fig. S3a). Peak $[Ca^{2+}]_c$ responses were reduced from 100% in the 1st pulse to 87.2 ± 3.8, 83.3 ± 6.5 and 58.71 ± 6.3% during the 2nd, 3rd, and 4th control pulse, respectively (Fig. S3c). Total calcium entry measured as the area under the curve of the $[Ca^{2+}]_c$ transients was reduced from 100% in the 1st pulse to 70.6 ± 9.1, 58.8 ± 5.6, 46.8 ± 9.1% in the 2nd, 3rd, and 4th control pulse, respectively (Fig. 3Sd).

When GPE (100 μM) was perfused starting 3 min before the 2nd pulse until two min after the 3rd pulse (Fig. S3b), the peak $[Ca^{2+}]_c$ responses were similar to the control responses (Fig. S3c). However, when total calcium entry was evaluated, GPE appeared to prevent inactivation of the depolarizing control response (Fig. S3d). This phenomenon can be attributed to the fact that GPE increased the inactivation constant of the K^+ induced $[Ca^{2+}]_c$ response from 19.8 s in control (P1) to 28.81 s in GPE treated cells (P3). After washout of the compound the inactivation constant returned to control values (14.85 s). In control cells the inactivation constant was maintained at similar values (Table 2).

Table 2 Values of the activation (τ_a) and inactivation constants (τ_i), in seconds, of the K^+ induced $[Ca^{2+}]_c$ responses in control cells (CONTROL) and cells treated with 100 μM GPE. P1, P2, P3, and P4 correspond to the 1st, 2nd, 3rd, and 4th consecutive 5 s K^+ pulses in hippocampal neurons

CONTROL	P1	P2	P3	P4
$\tau_{a\ (s)}$	4.88	4.35	3.50	4.08
$\tau_{I\ (s)}$	21.24	22.41	26.28	27.61
GPE	P1	P2 + GPE 100 μM	P3 + GPE 100 μM	P4-washout
$\tau_{a\ (s)}$	5.04	3.77	3.32	5.57
$\tau_{I\ (s)}$	19.89	26.44*	28.81*	14.87

*$p < 0.05$ compared with respective control.

Discussion

The key findings of this study are: (i) GPE administration, but not cPG, partially restores the decrease in both SRIF content and SRIF receptor density induced by Aβ25–35 infusion; (ii) inhibition of cell death after GPE administration to Aβ25–35-treated rats is coincident with activation of CREB and Akt and inhibition of GSK3β signaling; (iii) the effects induced by GPE are independent of Aβ25–35 clearance; and (iv) the protective effects of GPE may be related with modulation of intracellular calcium signaling, inhibition of glutamate binding to NMDA receptors and protection against NMDA excitotoxicity.

Our experimental model consisted in a continuous infusion of Aβ that induces the main changes described in AD patients such as Aβ deposits distributed throughout the cortex and changes in cognitive functions and neurotransmitter expression (Yamaguchi *et al.* 2006). In this study, Aβ25–35 was chosen because this fragment is proposed to be the functional domain of Aβ responsible for its neurotoxic properties and it is present in the brain of AD patients (Kubo *et al.* 2002).

Somatostatin neurons are more susceptible to Aβ toxicity than other neurons (Nag *et al.* 1999) and we previously reported increased death of SRIF-containing cells in response to Aβ25–35 (Aguado-Llera *et al.* 2007). Here and as previously reported, we demonstrate that Aβ25–35 decreases SRIF-LI levels, increases cell death and reduces p-Akt levels, in addition to decreasing the density of SRIF receptors. The latter appears to be selective for sst2 as the mRNA and protein content of only this receptor subtype was found to vary, similar to what is reported to occur in AD cortices (Kumar 2005). Our present results indicate that the toxic effects of Aβ25–35 may involve a reduction in p-CREB levels. As Aβ inhibits the CREB-signaling pathways (Vitolo *et al.* 2002) and the SRIF and sst2 genes contain cAMP responsive element (CRE) sites (Montminy and Bilezikjian 1987; Kimura *et al.* 2001), Aβ25–35 may reduce SRIF and sst2 mRNA levels through CREB inhibition.

Infusion of Aβ25–35 did not change basal AC activity. However, the capacity of SRIF to inhibit AC activity was lower in Aβ25–35-treated rats. This could be due to the reduction in sst2, as the relationship between the reduction in

SRIF receptor density and the lower inhibitory effect of SRIF on AC activity has been described in AD patients (Cowburn *et al.* 1991). Thus, the physiological consequences of this decrease may be related with attenuated intracellular signaling, as we have shown here. In fact, SRIF receptors are negatively coupled to AC via G proteins and this pathway is partially responsible for the sst2 receptor-mediated modulation of intracellular calcium levels (Cervia *et al.* 2002).

Although IGF-I is a physiological regulator of Aβ levels (Carro *et al.* 2002), GPE and cPG do not modulate brain Aβ25–35 levels. However, GPE was able to partially block the Aβ-induced changes in SRIF and sst2. This result indicates that GPE and IGF-I exert at least part of their effects through distinct mechanisms and indeed, GPE fails to bind either IGF-I or IGF-II receptors (Sara *et al.* 1993).

Glycine-proline-glutamate could inhibit the decline in SRIF and sst2 by increasing the survival of cells that express these proteins and/or stimulation of their expression in individual cells. Indeed, peripheral administration of GPE increased cortical levels of p-CREB in Aβ-treated rats, and SRIF and sst2 gene transcription is enhanced by the binding of p-CREB to cAMP responsive element (CRE) sites in these genes (Mayr and Montminy 2001). In addition, GPE increases Akt phosphorylation, which can increase cell survival via activation of CREB (Chong *et al.* 2005). Thus, it is possible that GPE could increase CREB phosphorylation via the Akt pathway, counteracting the effects of Aβ25–35 on SRIF and sst2 expression, as well as on cell survival. Indeed, we have shown that GPE, but not cPG, interacts with NMDA receptors, displacing glutamate from these binding sites. Neuroprotective mechanisms that inactivate NMDA receptors with a parallel activation of PI3K/Akt pathway have been described (Chuang 2005). Our results suggest that the glutamate residue may be important in the mechanism of action of this tripeptide, given that cPG neither displaced glutamate nor activated this pathway, suggesting that GPE may act as a NMDA receptor antagonist. In support of this, previous studies demonstrated that changes made at the C-terminal glutamate residue resulted in inactive compounds (Brimble *et al.* 2005).

Binding of IGF-I to its receptor activates Akt, which can then phosphorylate GSK3β on serine 9, resulting in its inhibition. Here we demonstrate that the IGF-I metabolite GPE inactivates the pro-apoptotic protein GSK3β in Aβ25–35-treated rats, through phosphorylation of its serine 9 residue. On the contrary, Tyr216 phosphorylation increases the activity of this enzyme (Grimes and Jope 2001). Indeed, Aβ-administration increased phosphorylation of GSK3β on Tyr216, as previously reported to occur in response to other apoptotic stimuli (Bhat *et al.* 2000), and GPE was able to block this effect. The inactivation of GSK3β by GPE, through both decreasing it phosphorylation on Tyr216 and increasing Ser9 phosphorylation, has a highly potential clinical application, given that increased GSK3 activity promotes inflammation in AD and contributes to Aβ-mediated neuronal death (Jope *et al.* 2007).

Neither Aβ25–35 nor GPE change HSP27 or p53 levels. Expression of HSP27 is associated with the presence of classic senile plaques, whereas other HSPs are present in diffuse plaques (Yokota *et al.* 2006). However, HSP27 levels may not be induced by Aβ25–35, as this protein forms protofibrils rather than large amyloid fibrils (Liu *et al.* 2004). Although p53 accumulates in cells of AD brain, inactivation of this protein does not modify Aβ25–35 induced cell death, demonstrating that this fragment induces apoptosis in a p53-independent manner (Blasko *et al.* 2000). The lack of changes in ERK1/2 indicates that the survival properties of GPE are most probably not mediated through this pathway, in agreement with what has been reported for IGF-I (Zheng and Quirion 2004). Nevertheless, the effect of other Aβ fragments on ERK1/2 activation is unclear. Activation of ERK1/2 has been reported in some AD models, but this effect is mainly with Aβ oligomers with higher molecular weight than Aβ25–35 (Chong *et al.* 2006); however this point remains controversial as lack of change or inhibition have also been reported (Damjanac *et al.* 2008; Mok *et al.* 2006).

Growing evidence indicates that Aβ increases calcium influx into neurons inducing cell death by apoptosis. Aβ peptides can insert into the membrane and form ion channels

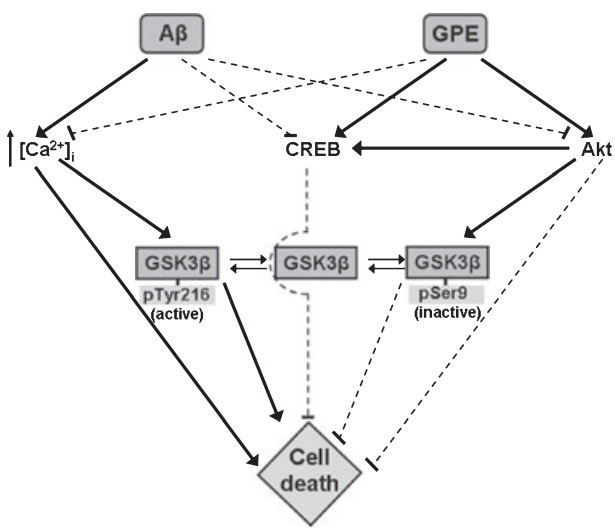

Fig. 3 Proposed mechanism of action. Phosphorylation-dependent regulation of GSK3β by GPE may antagonize apoptotic effects of Aβ. Protective effects of GPE may be related with activation (solid arrow) of survival signaling pathways (Akt and CREB) and blockage (dashed line) of proapoptotic signals, as an increase of cytosolic calcium concentrations ($[Ca^{2+}]_c$). Phosphorylation of Akt inactivates GSK3β by serine phosphorylation, reducing cell death. In turn, a raise of $[Ca^{2+}]_c$ may activate GSK3β by tyrosine phosphorylation, increasing cell death. Aβ, beta-amyloid; CREB, cAMP-responsive element binding protein; GPE, Gly-Pro-Glu; GSK3β, glycogen synthase kinase 3β.

or alter the activity of glutamate receptors, modulating calcium influx (Shankar *et al.* 2007). Indeed, Aβ25–35 induces apoptosis in cultured neurons that is associated with an increase in $[Ca^{2+}]_c$ (Zeng *et al.* 2004). We have chosen hippocampal neurons, given that in culture these neurons are more vulnerable than cortical neurons to Aβ25–35 by a mechanism that involves perturbation of calcium homeostasis (Resende *et al.* 2007). Because GPE modulates NMDA receptor activity (Sara *et al.* 1993), it could regulate calcium influx and reduce glutamate-induced cytotoxicity (Brewer *et al.* 2007), through a mechanism that may involve GSK3β inactivation. Indeed, increases of $[Ca^{2+}]_c$ are closely associated with tyrosine phosphorylation of GSK3β (Hartigan and Johnson 1999) and here we show that GPE significantly reduces the glutamate induced elevation in $[Ca^{2+}]_c$. Although excessive elevation of $[Ca^{2+}]_c$ is a trigger of neuronal injury in AD, moderate increases of $[Ca^{2+}]_c$ are required for activation of anti-apoptotic proteins (Bickler and Fahlman 2004), as well as for pro-SRIF formation (Austin and Shields 1996). A slight increase in $[Ca^{2+}]_c$ after GPE incubation, as demonstrated in this report, could be associated with Akt activation and CREB phosphorylation (Yano *et al.* 2005). These results are in accordance with the lack of effect of cPG on $[Ca^{2+}]_c$ after incubation. Finally, GPE did not modify the peak $[Ca^{2+}]_c$ increase induced by K^+, but did increase total calcium entry measured as the area under the curve. Our interpretation is that GPE does not affect voltage-dependent calcium channels since we observe no differences in $[Ca^{2+}]_c$ peaks, but could be inducing release from intracellular calcium deposits as shown by $[Ca^{2+}]_c$ signals when GPE was given alone and because it increased the inactivation constant of the $[Ca^{2+}]_c$ transient caused by high K^+.

In summary, the present study demonstrates an *in vivo* protective effect of GPE on the SRIF system in the temporal cortex of Aβ25–35-treated rats. The protective action of GPE in the temporal cortex, independent of Aβ clearance, may antagonize deleterious effects of Aβ through Akt activation, which could reduce GSK3β signaling by Ser9 phosphorylation and Tyr216 dephosphorylation (Fig. 3). In addition, *in vitro* GPE shows a protective effect by lowering $[Ca^{2+}]_c$ after glutamate insult, but in the basal state promotes a moderate elevation of $[Ca^{2+}]_c$ compatible with neuroprotective processes. The activation of the mentioned protective pathways, together with the blockage of apoptotic signaling, indicates that GPE acts as a survival factor against Aβ insult in brain. These findings contribute to the understanding of the mechanisms involved in GPE neuroprotection and suggest a possible new therapeutic strategy for AD.

Acknowledgements

The authors wish to thank Dr Julie A. Chowen for the critical review of the manuscript, Dr Ignacio Torres-Alemán for the advising on the immunoprecipitation technique and Sandra Canelles for the technical support. This work was supported by grants of Fondo de Investigación Sanitaria (CD07/00256 to EBR and CM05/00100 to GAMM), Spanish Ministery of Education (SAF2006-08540), CIBERobn, RETICS-RD06/0026, Instituto de Salud Carlos III, Comunidad Autónoma de Madrid (SAL2006/0275) and Fundación Endocrinología y Nutrición.

Supporting Information

Additional Supporting Information may be found in the online version of this article:

Figure S1 Levels of β-amyloid-25-35 (Aβ25–35) in the temporal cortex from control ovariectomized (C-Ovx) rats, C-Ovx rats treated with β-amyloid 25–35 peptide (Aβ25–35), C-Ovx rats treated with Aβ25–35 plus Gly-Pro-Glu (Aβ25–35 + GPE), C-Ovx rats treated with Aβ25–35 plus cyclo[Pro-Glu] (Aβ25–35 + cPG), C-Ovx rats treated with GPE alone and C-Ovx rats treated with cPG alone.

Figure S2 (a–d) TUNEL-positive cells (green) in the temporal cortex of C-Ovx rats (a), C-Ovx rats treated with Aβ25–35 (b), C-Ovx rats treated with Aβ25–35 + GPE (c) and C-Ovx rats treated with GPE alone (d).

Figure S3 Inhibitory effect of GPE on 70 mM K^+-induced $[Ca^{2+}]_c$ elevation in cultured hippocampal neurons.

Please note: Wiley-Blackwell are not responsible for the content or functionality of any supporting materials supplied by the authors. Any queries (other than missing material) should be directed to the corresponding author for the article.

References

Aguado-Llera D., Martín-Martínez M., García-López M. T., Arilla-Ferreiro E. and Barrios V. (2004) Gly-Pro-Glu protects β-amyloid-induced somatostatin depletion in the rat cortex. *Neuroreport* **15**, 1979–1982.

Aguado-Llera D., Arilla-Ferreiro E., Chowen J. A., Argente J., Puebla-Jiménez L., Frago L. M. and Barrios V. (2007) 17β-estradiol protects depletion of rat temporal cortex somatostatinergic system by β-amyloid. *Neurobiol. Aging* **28**, 1396–1409.

Austin C. D. and Shields D. (1996) Prosomatostatin processing in permeabilized cells. Calcium is required for prohormone cleavage but not formation of nascent secretory vesicles. *J. Biol. Chem.* **271**, 1194–1199.

Bhat R. V., Shanley J., Correll M. P., Fieles W. E., Keith R. A., Scott C. W. and Lee C. M. (2000) Regulation and localization of tyrosine216 phosphorylation of glycogen synthase kinase-3beta in cellular and animal models of neuronal degeneration. *Proc. Natl Acad. Sci. USA* **97**, 11074–11079.

Bickler P. E. and Fahlman C. S. (2004) Moderate increases in intracellular calcium activate neuroprotective signals in hippocampal neurons. *Neuroscience* **127**, 673–683.

Blasko I., Wagner M., Whitaker N., Grubeck-Loebenstein B. and Jansen-Durr P. (2000) The amyloid beta peptide abeta (25–35) induces apoptosis independent of p53. *FEBS Lett.* **470**, 221–225.

Brewer L. D., Thibault O., Staton J., Thibault V., Rogers J. T., García-Ramos G., Kraner S., Landfield P. W. and Porter N. M. (2007) Increased vulnerability of hippocampal neurons with age in culture: temporal association with increases in NMDA receptor current, NR2A subunit expression and recruitment of L-type calcium channels. *Brain Res.* **1151**, 20–31.

Brimble M. A., Trotter N. S., Harris P. W. and Sieg F. (2005) Synthesis and pharmacological evaluation of side chain modified glutamic acid analogues of the neuroprotective agent glycyl-L-prolyl-L-glutamic acid (GPE). *Bioorg. Med. Chem.* **13**, 519–532.

Carro E., Trejo J. L., Gómez-Isla T., LeRoith D. and Torres-Alemán I. (2002) Serum insulin-like growth factor I regulates brain amyloid-beta levels. *Nat. Med.* **8**, 1390–1397.

Cervia D., Fiorini S., Pavan B., Biondi C. and Bagnoli P. (2002) Somatostatin (SRIF) modulates distinct signaling pathways in rat pituitary tumor cells; negative coupling of SRIF receptor subtypes 1 and 2 to arachidonic acid release. *Naunyn Schmiedebergs Arch. Pharmacol.* **365**, 200–209.

Chomczynski P. (1993) A reagent for the single-step simultaneous isolation of RNA, DNA and proteins from cell and tissue samples. *BioTechniques* **15**, 532–537.

Chong Z. Z., Li F. and Maiese K. (2005) Activating Akt and the brain's resources to drive cellular survival and prevent inflammatory injury. *Histol. Histopathol.* **20**, 299–315.

Chong Y. H., Shin Y. J., Lee E. O., Kayed R., Glabe C. G. and Tenner A. J. (2006) ERK1/2 activation mediates Abeta oligomer-induced neurotoxicity via caspase-3 activation and tau cleavage in rat organotypic hippocampal slice cultures. *J. Biol. Chem.* **281**, 20315–20325.

Chuang D. M. (2005) The antiapoptotic actions of mood stabilizers: molecular mechanisms and therapeutic potentials. *Ann. NY Acad. Sci.* **1053**, 195–204.

Cowburn R. F., Fowler C. J., Garlind A., Alafuzoff I., Nilsson L., Winblad B. and Bergstrom L. (1991) Somatostatin receptors and the modulation of adenylyl cyclase activity in Alzheimer′s disease. *J. Neurol. Neurosurg. Psych.* **54**, 748–749.

Damjanac M., Rioux-Bilan A., Paccalin M., Pontcharraud R., Fauconneau B., Hugon J. and Page G. (2008) Dissociation of Akt/PKB and ribosomal S6 kinase signaling markers in a transgenic mouse model of Alzheimer's disease. *Neurobiol. Dis.* **29**, 354–367.

Figueredo-Cardenas G., Anderson K. D., Chen Q., Veenman C. L. and Reiner A. (1994) Relative survival of striatal projection neurons and interneurons after intrastriatal injection of quinolinic acid in rats. *Exp. Neurol.* **129**, 37–56.

Foster A. C. and Fagg G. E. (1987) Comparison of L-[3H]glutamate, D-[3H]aspartate, DL-[3H]AP5 and [3H]NMDA as ligands for NMDA receptors in crude postsynaptic densities from rat brain. *Eur. J. Pharmacol.* **133**, 291–300.

Gilman A. G. (1970) A protein binding assay for adenosine 3′5′-cyclic monophosphate. *Proc. Natl Acad. Sci. USA* **67**, 305–312.

Górecki D. C., Beresewicz M. and Zablocka B. (2007) Neuroprotective effects of short peptides derived from the insulin-like growth factor 1. *Neurochem. Int.* **51**, 451–458.

Grimes C. A. and Jope R. S. (2001) The multifaceted roles of glycogen synthase kinase 3β in cellular signaling. *Prog. Neurobiol.* **65**, 391–426.

Grynkiewicz G., Poenie M. and Tsien R. Y. (1985) A new generation of Ca^{2+} indicators with greatly improved fluorescence properties. *J. Biol. Chem.* **260**, 3440–3450.

Guan J., Thomas G. B., Lin H., Mathai S., Bachelor D. C., George S. and Gluckman P. D. (2004) Neuroprotective effects of the N-terminal tripeptide of insulin-like growth factor-1, glycine-proline-glutamate (GPE) following intravenous infusion in hypoxic-ischemic adult rats. *Neuropharmacology* **47**, 892–903.

Hartigan J. A. and Johnson G. V. (1999) Transient increases in intracellular calcium result in prolonged site-selective increases in Tau phosphorylation through a glycogen synthase kinase 3β-dependent pathway. *J. Biol. Chem.* **274**, 21395–21401.

Hynd M. R., Scott H. L. and Dodd P. R. (2004) Glutamate-mediated excitotoxicity and neurodegeneration in Alzheimer's disease. *Neurochem. Int.* **45**, 583–595.

Jope R. S., Yuskaitis C. J. and Beurel E. (2007) Glycogen synthase kinase-3 (GSK3): inflammation, diseases, and therapeutics. *Neurochem. Res.* **32**, 577–595.

Khan S. S., Smith M. S., Reda D., Suffredini A. F. and McCoy J. P. Jr (2004) Multiplex bead array assays for detection of soluble cytokines: comparisons of sensitivity and quantitative values among kits from multiple manufacturers. *Cytometry B. Clin. Cytom.* **61**, 35–39.

Kimura N., Tomizawa S., Arai K. N., Osamura R. Y. and Kimura N. (2001) Characterization of 5′-flanking region of rat somatostatin receptor sst2 gene: transcriptional regulatory elements and activation by Pitx1 and estrogen. *Endocrinology* **142**, 1427–1441.

Koh J. Y. and Choi D. W. (1987) Quantitative determination of glutamate mediated cortical neuronal injury in cell culture by lactate dehydrogenase efflux assay. *J. Neurosci. Methods* **20**, 83–90.

Kubo T., Nishimura S., Kumagae Y. and Kaneko I. (2002) In vivo conversion of racemized beta-amyloid ([D-Ser 26]A beta 1–40) to truncated and toxic fragments ([D-Ser 26]A beta 25–35/40) and fragment presence in the brains of Alzheimer's patients. *J. Neurosci. Res.* **70**, 474–483.

Kumar U. (2005) Expression of somatostatin receptor subtypes (SSTR1–5) in Alzheimer's disease brain: an immunohistochemical analysis. *Neuroscience* **134**, 525–538.

Liu R., McAllister C., Lyubchenko Y. and Sierks M. R. (2004) Residues 17–20 and 30–35 of beta-amyloid play critical roles in aggregation. *J. Neurosci. Res.* **75**, 162–171.

Mayr B. and Montminy M. (2001) Transcriptional regulation by the phosphorylation-dependent factor CREB. *Nat. Rev. Mol. Cell Biol.* **2**, 599–609.

Mok S. S., Losic D., Barrow C. J., Turner B. J., Masters C. L., Martin L. L. and Small D. H. (2006) The beta-amyloid peptide of Alzheimer's disease decreases adhesion of vascular smooth muscle cells to the basement membrane. *J. Neurochem.* **96**, 53–64.

Monahan J. B. and Michel J. (1987) Identification and characterization of an N-methyl-D-aspartate-specific L-[3H]glutamate recognition site in synaptic plasma membranes. *J. Neurochem.* **48**, 1699–1708.

Montminy M. R. and Bilezikjian L. M. (1987) Binding of a nuclear protein to the cyclic-AMP response element of the somatostatin gene. *Nature* **328**, 175–178.

Nag S., Yee B. K. and Tang F. (1999) Reduction in somatostatin and substance P levels and choline acetyltransferase activity in the cortex and hippocampus of the rat after chronic intracerebroventricular infusion of β-amyloid (1–40). *Brain Res. Bull.* **50**, 251–262.

Patel Y. C. and Reichlin S. (1978) Somatostatin in hypothalamus, extrahypothalamic brain and peripheral tissues of the rat. *Endocrinology* **102**, 523–530.

Quevedo C., Alcázar A. and Salinas M. (2000) Two different signal transduction pathways are implicated in the regulation of initiation factor 2B activity in insulin-like growth factor-1-stimulated neuronal cells. *J. Biol. Chem.* **275**, 19192–19197.

Reinikainen K. J., Soininen H. and Riekkinen P. J. (1990) Neurotransmitter changes in Alzheimer's disease: implications to diagnostics and therapy. *J. Neurosci. Res.* **27**, 576–586.

Reisine T. and Bell G. I. (1995) Molecular biology of somatostatin receptors. *Endocrinol. Rev.* **16**, 427–442.

Resende R., Pereira C., Agostinho P., Vieira A. P., Malva J. O. and Oliveira C. R. (2007) Susceptibility of hippocampal neurons to Aβ peptide toxicity is associated with perturbation of Ca^{2+} homeostasis. *Brain Res.* **1143**, 11–21.

Reubi J. C., Perrin M. H., Rivier J. E. and Vale V. (1981) High affinity binding sites for the somatostatin-28 analogue in rat brain. *Life Sci.* **28**, 2191–2198.

Sara V. R., Carlsson-Skwirut C., Drakenberg K. *et al.* (1993) The biological role of truncated insulin-like growth factor-1 and the trip-

eptide GPE in the central nervous system. *Ann. NY Acad. Sci.* **692**, 183–191.

Shankar G. M., Bloodgood B. L., Townsend M., Walsh D. M., Selkoe D. J. and Sabatini B. L. (2007) Natural oligomers of the Alzheimer amyloid-beta protein induce reversible synapse loss by modulating an NMDA-type glutamate receptor-dependent signaling pathway. *J. Neurosci.* **27**, 2866–2875.

Sizonenko S. V., Sirimanne E. S., Williams C. E. and Gluckman P. D. (2001) Neuroprotective effects of the N-terminal tripeptide of IGF-1, glycine-proline-glutamate, in the immature rat brain after hypoxic-ischemic injury. *Brain Res.* **922**, 42–50.

Snider B. J., Moss J. L., Revilla F. J., Lee C. S., Wheeler V. C., Macdonald M. E. and Choi D. W. (2003) Neocortical neurons cultured from mice with expanded CAG repeats in the huntingtin gene: unaltered vulnerability to excitotoxins and other insults. *Neuroscience* **120**, 617–625.

Takashima A. (2006) GSK-3 is essential in the pathogenesis of Alzheimer's disease. *J. Alzheimers Dis.* **9** (Suppl. 3), 309–317.

Vitolo O. V., Sant'Angelo A., Costanzo V., Battaglia F., Arancio O. and Shelanski M. (2002) Amyloid beta-peptide inhibition of the PKA/CREB pathway and long-term potentiation: reversibility by drugs that enhance cAMP signaling. *Proc. Natl Acad. Sci. USA* **99**, 13217–13221.

Walsh D. M. and Selkoe D. J. (2004) Deciphering the molecular basis of memory failure in Alzheimer's disease. *Neuron* **44**, 181–193.

Williamson R., Scales T., Clark B. R. *et al.* (2002) Rapid tyrosine phosphorylation of neuronal proteins including tau and focal adhesion kinase in response to amyloid-beta peptide exposure: involvement of Src family protein kinases. *J. Neurosci.* **22**, 10–20.

Yamaguchi Y., Miyashita H., Tsunekawa H., Mouri A., Kim H. C., Saito K., Matsuno T., Kawashima S. and Nabeshima T. (2006) Effects of a novel cognitive enhancer, spiro[imidazo-[1,2-a]pyridine-3,2-indan]-2(3H)-one (ZSET1446), on learning impairments induced by amyloid-beta1–40 in the rat. *J. Pharmacol. Exp. Ther.* **317**, 1079–1087.

Yano S., Morioka M., Kuratsu J. and Fukunaga K. (2005) Functional proteins involved in regulation of intracellular Ca(2+) for drug development: role of calcium/calmodulin-dependent protein kinases in ischemic neuronal death. *J. Pharmacol. Sci.* **97**, 351–354.

Yokota T., Mishra M., Akatsu H. *et al.* (2006) Brain site-specific gene expression analysis in Alzheimer's disease patients. *Eur. J. Clin. Invest.* **36**, 820–830.

Zeng H., Chen Q. and Zhao B. (2004) Genistein ameliorates β-amyloid peptide (25–35)-induced hippocampal neuronal apoptosis. *Free Radic. Biol. Med.* **36**, 180–188.

Zheng W. H. and Quirion R. (2004) Comparative signaling pathways of insulin-like growth factor-1 and brain-derived neurotrophic factor in hippocampal neurons and the role of the PI3 kinase pathway in cell survival. *J. Neurochem.* **89**, 844–852.

Zheng H., Xu H., Uljon S. N. *et al.* (2002) Modulation of Aβ peptides by estrogen in mouse models. *J. Neurochem.* **80**, 191–196.

